by an X-ray diffraction study (Figure 1).[8] This is the first X-ray crystal structure of an exo-[$2_\sigma + 2_\sigma + 2_\pi$] cycloadduct of quadricyclane with a double-bonded π-partner. There is little distortion in the bicyclo[2.2.1]heptene system while the planar silacyclobutane shows remarkable features. The smallest endocyclic angle, C1-Si2-C7, is 81.39°, and the largest, C1-C2-C7, is 102.2°. Bonds in the ring are elongated; the Si2···C2 distance is shorter than C1···C7. Steric interaction is mirrored by bond angles only.

Intramolecular [1,3] rearrangements in silene chemistry are known.[9] We propose that the rearrangement **2** → **3** occurs by primary nucleophilic attack of the oxygen on the silene silicon atom, thus resembling an intramolecular base stabilized silene, followed by a transition state with a bridging *tert*-butoxy group (Scheme II), and finally full migration to yield **3**.

Acknowledgment. We thank Stiftung Volkswagenwerk, Deutsche Forschungsgemeinschaft, and Fonds der Chemischen Industrie for support.

Registry No. 1, 141248-12-6; **2**, 141248-13-7; **3**, 141248-14-8; **4b**, 141248-15-9; **5**, 141248-16-0; **6**, 141248-17-1; **7**, 141248-18-2; **8**, 141248-19-3; $(CH_2{=}CH)ScMe_2(OBu^t)$, 5507-47-1; $Me_2SiCl(CH{=}CH_2)$, 1719-58-0; $(BrCH{=}CBr)SiMe_2(OBu^t)$, 141248-20-6; $(CH_2{=}CBr)SiMe_2(OBu^t)$, 141248-21-7; $Me_2Si(OBu^t)C((OMe)_3Si){=}CH_2$, 141248-22-8; $Et_2SiCl(CH{=}CH_2)$, 15972-93-7; $Et_2Si(OPr^i)(CH{=}CH_2)$, 141248-23-9; $Et_2Si(OPr^i)(CBr{=}CH_2)$, 141248-24-0; Me_3SiOMe, 1825-61-2; quadricyclane, 278-06-8.

Supplementary Material Available: Tables of bond lengths, bond angles, positional parameters, and thermal parameters for **6** and experimental and analytical data (17 pages); listing of observed and calculated structure factors for **6** (18 pages). Ordering information is given on any current masthead page.

(7) Haselbach, E.; Martin, H.-D. *Helv. Chim. Acta* **1974**, *57*, 472.

(8) **6** ($C_{19}H_{34}Cl_2OSi_2$): space group $P\bar{1}$ (Int. Tables 2), a = 8.672 (3) Å, b = 9.463 (3) Å, c = 14.074 (5) Å, α = 89.25 (2)°, β = 88.50°, γ = 86.55 (2)°, V = 1152 Å^3, Z = 2, μ(Mo Kα) = 3.9 cm^{-1}; Enraf-Nonius CAD-4 diffractometer (graphite monochromator); 3630 unique reflections collected ($2° < 2\theta < 50°$); 2958 reflections considered observed ($I > \sigma(I)$), used to solve (direct methods) and refine (least squares). R and R_w: 0.055 and 0.043.

(9) Eaborn, C.; Happer, D. A. R.; Hitchcock, P. B.; Hopper, S. P.; Safa, K. D.; Washburne, S. S.; Walton, D. R. M. *J. Organomet. Chem.* **1980**, *186*, 309. Wiberg, N.; Köpf, H. *Chem. Ber.* **1987**, *120*, 653. Ishikawa, M.; Nishimura, K.; Ochiai, H.; Kumada, M. *J. Organomet. Chem.* **1982**, *236*, 7. Ando, W.; Sekiguchi, A.; Sato, T. *J. Am. Chem. Soc.* **1981**, *103*, 5573.

Ordered Oxygen on Mo(112): Modification of Surface Electronic Structure and Control of Reaction Path

Tetsuya Aruga, Ken-ichi Fukui, and Yasuhiro Iwasawa*

Department of Chemistry, Faculty of Science
The University of Tokyo
Hongo, Bunkyo-ku, Tokyo 113, Japan

Received January 22, 1992

It has been a long-sought goal in chemistry to design an active and selective catalyst for each particular reaction. This requires knowledge of the microscopic principle of surface modification and various means to modify the electronic structure and the steric confinement of the surface. We have studied the oxygen modification of the Mo(112) surface. On the Mo(112)-p(1×1) surface (Figure 1), oxygen atoms are expected to occupy trough sites. We have succeeded in controlling the electronic structure of the first-layer Mo atoms as probed directly by the CO adsorption. We have also succeeded in selectively blocking the second-layer Mo atoms. High-coordination metal sites exhibit high electronic fluctuation and are believed to play a major role in structure-sensitive catalytic reactions.[1] The blocking of the second-layer

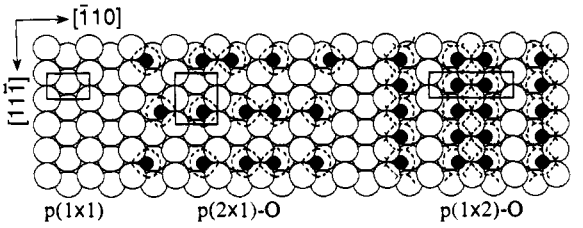

Figure 1. Models for the Mo(112)-p(1×1), Mo(112)-p(2×1)-O, and Mo(112)-p(1×2)-O surfaces. The van der Waals spheres of O atoms are shown by the dotted lines.

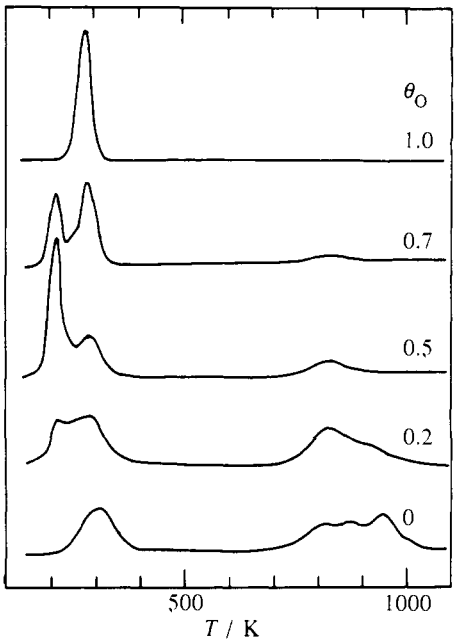

Figure 2. TPD traces of CO from clean and O-precovered Mo(112). Desorption peaks above 800 K are due to dissociatively adsorbed CO.[2]

atoms resulted in a new methanol dehydrogenation path, unlike the oxidative dehydrogenation usually observed on molybdenum oxides.

The low-energy electron diffraction experiments after exposure of clean Mo(112) at 300 K to oxygen followed by annealing to 600 K showed a series of ordered structures, p(2×1)-O at θ_O = 0.5, p(1×2)-O at θ_O = 1.0, and four intermediate phases,[2] where θ_O denotes the oxygen coverage. Figure 2 shows the results of temperature-programmed desorption (TPD) of CO from O-precovered Mo(112). CO adsorbed molecularly on clean Mo(112) gives rise to a desorption peak (α_1) at 310 K. With increasing θ_O, this peak decreases in intensity and shifts to 280 K, while a new peak (α_2) appears at 220 K. The α_1:α_2 ratio reaches 1:2 at θ_O = 0.5 (p(2×1) surface), beyond which α_2 is again suppressed and α_1 regrows. The α_2 peak disappears completely at θ_O = 1.0 (p(1×2) surface).

We suppose that O(a) on Mo(112) occupies a quasi-3-fold hollow site composed of one second-layer and two first-layer Mo atoms on the basis of the result of an ion-scattering study for O/W(112).[3] The models for Mo(112)-p(2×1)-O and Mo(112)-p(1×2)-O are shown in Figure 1. There are two equivalent quasi-3-fold sites in a p(1×1) unit mesh. If all O(a) atoms occupy the sites in the same side, it is difficult to explain the two CO desorption peaks from p(2×1)-O. We, therefore, suppose that each O(a) occupies either of the two equiprobable sites randomly.[4] This causes three types of top-layer Mo atoms to be formed on p(2×1)-O: those coordinated by two O(a) atoms (Mo_{2C}), those

(1) Falicov, L. M.; Somorjai, G. A. *Proc. Natl. Acad. Sci. U.S.A.* **1985**, *82*, 2207.

(2) Fukui, K.; Aruga, T.; Iwasawa, Y. To be published.

(3) Bu, H.; Grizzi, O.; Shi, M.; Rabalais, J. W. *Phys. Rev. B* **1989**, *40*, 10147.

(4) A model calculation showed that this structure gives rise to a slightly weak but sharp p(2×1) diffraction pattern.

0002-7863/92/1514-4911$03.00/0

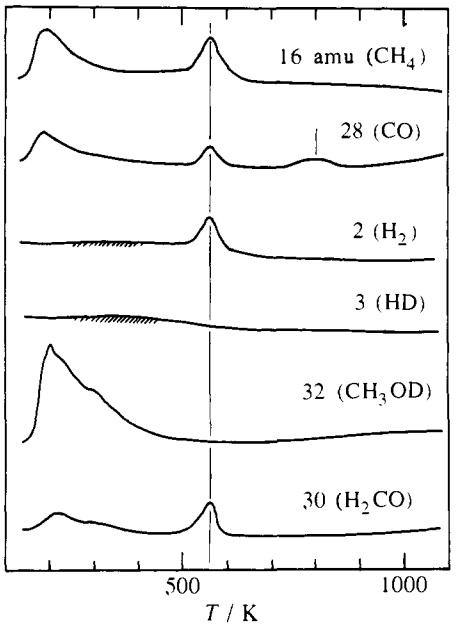

Figure 3. TPD traces measured after exposure of Mo(112)-p(1×2)-O at 130 K to 4 langmuirs of CH_3OD.

coordinated by one O(a) atom (Mo_{1C}), and those not coordinated (Mo_{NC}), the ratio of the three being 1:2:1. Considering the van der Waals radius[5] of O atoms, it is expected that CO cannot be adsorbed on Mo_{2C} but can be adsorbed on Mo_{1C} and Mo_{NC}. The α_1- and α_2-CO species are then assigned to CO adsorbed on Mo_{NC} and Mo_{1C}, respectively. This assignment applies also to CO TPD from p(1×2)-O, where Mo_{NC} and Mo_{4C} coexist and only α_1-CO is observed.

The desorption energies of α_1- and α_2-CO are estimated to be 72 and 56 kJ mol^{-1}, respectively.[6] The difference, 16 kJ mol^{-1}, is ascribed to the electronic effect of one O modifier, since the steric blocking is negligible for Mo_{1C}. This electronic effect is restricted to Mo atoms directly coordinated by O(a) and can be explained in terms of the withdrawal of electrons by electronegative O(a). On the other hand, the gradual shift of the CO desorption peaks, from 310 to 280 K for α_1, is ascribed to a long-range electronic effect due to the rearrangement of surface electronic states extending to several lattice spacings.[7]

The TPD measurement after exposure of clean Mo(112) at 130 K to CH_3OD showed desorption-limited peaks of HD and H_2 at 380 K and a sharp desorption peak of H_2 at 410 K, suggesting that CH_3OD dissociates to methoxy (CH_3O(a)) and D(a) at low temperatures. D(a) is recombinatively desorbed with H(a) adsorbed from the residual gas. CH_3O(a) is decomposed at 410 K to form H_2(g), C(a), and O(a). The C(a) and O(a) species are desorbed above 800 K as CO, in contrast to the cases of many transition metal surfaces,[8] where the reaction-limited, simultaneous desorption of CO and H_2 is observed. A small amount of CH_4 is also desorbed at 450 K. These results indicate that the C-O bond scission competes well with the C-H scission on clean Mo(112).

A remarkably different reaction path is opened on p(1×2)-O, whereas the TPD results for p(2×1)-O are practically identical to those for clean Mo(112). Figure 3 shows TPD measured after exposure of the p(1×2)-O surface to CH_3OD. Simultaneous desorption of H_2CO, H_2, CO, and CH_4 is observed at 560 K, below which only hydrogen desorbs at 300-400 K. The desorption at 560 K does not contain deuterated species, indicating that CH_3O(a) is formed also on p(1×2)-O at low temperatures and is decomposed at 560 K. The shift of the decomposition temperature by 150 K suggests the stabilization of CH_3O(a) on p(1×2)-O.

On molybdenum oxide catalysts, the oxidative dehydrogenation of CH_3OH occurs to form H_2CO and H_2O.[9,10] By contrast, a dehydrogenation path to produce H_2CO and H_2 is newly opened on Mo(112)-p(1×2)-O. The desorbed products from p(1×2)-^{18}O did not contain ^{18}O-labeled species, indicating that O(a) plays only a role as a modifier. The amount of C(a) and O(a) formed during the methoxy decomposition was small compared with the case of low-θ_O surfaces, suggesting that the C-O bond scission is restrained on p(1×2)-O. We suggest that the CH_3O(a) decomposition on p(1×2)-O is triggered by the C-H scission, since the simultaneous desorption peaks shifted upward by 10 K when CD_3OD was used. The CO adsorption experiments indicated that the electronic structure of top-layer Mo_{NC} atoms is identical for both p(2×1)-O and p(1×2)-O. The suppression of the C-O bond scission on p(1×2)-O is then ascribed to the steric blocking by O(a) of second-layer Mo, which plays an essential role in the C-O bond cleavage.

Registry No. Mo, 7439-98-7; CO, 630-08-0; O, 17778-80-2; CH_3OH, 67-56-1; molybdenum oxide, 11098-99-0.

(5) Bondi, A. *J. Phys. Chem.* **1964**, *68*, 441.
(6) The preexponential factor for desorption was assumed to be 10^{13} s^{-1}.
(7) Feibelman, P. J.; Hamann, D. R. *Phys. Rev. Lett.* **1984**, *52*, 61.
(8) Parmeter, J. E.; Jiang, X.; Goodman, D. W. *Surf. Sci.* **1990**, *240*, 85 and references therein.
(9) Farneth, W. E.; Ohuchi, F.; Staley, R. H.; Chowdhry, U.; Sleight, A. W. *J. Phys. Chem.* **1985**, *89*, 2493.
(10) Iwasawa, Y. *Adv. Catal.* **1987**, *35*, 87.

Stereoselective Hydrogen-Transfer Reactions Involving Acyclic Radicals. A Study of Radical Conformations Using Semiempirical Calculations

K. Durkin and D. Liotta*

Department of Chemistry, Emory University
1515 Pierce Drive, Atlanta, Georgia 30322

J. Rancourt,[†] J.-F. Lavallée,[†] L. Boisvert,[‡] and Y. Guindon[†,‡]

Bio-Méga Inc., 2100 rue Cunard
Laval, Québec, Canada H7S 2G5
Department of Chemistry, Université de Montréal
Montréal, Québec, Canada H3C 3J7
Received February 20, 1992

Stereoselectivity in intermolecular reactions of acyclic free radicals is a topic of current interest in chemical literature.[1] Recent reports show that chirality transfer can be achieved using stereogenic centers adjacent to a radical center.[2-4] The theoretical interpretation of these results being at an early stage, we have been developing a transition-state model that would account for the stereocontrol noted when radicals of low SOMO energy are

[†] Bio-Méga Inc.
[‡] Université de Montréal.
(1) Porter, N. A.; Giese, B.; Curran, D. P. *Acc. Chem. Res.* **1991**, *24*, 296 and references cited therein.
(2) (a) Hart, D. J.; Huang, H.-C. *Tetrahedron Lett.* **1985**, *26*, 3749. (b) Hart, D. J.; Krishnamurthy, R. *Synlett* **1991**, 412. (c) Hart, D. J.; Huang, H.-C.; Krishnamurthy, R.; Schwartz, T. *J. Am. Chem. Soc.* **1989**, *111*, 7507. (d) Hart, D. J.; Krishnamurthy, R. Submitted for publication (personal communication).
(3) (a) Bullard, M.; Zeitz, H.-G.; Giese, B. *Synlett* **1991**, 423. (b) Giese, B.; Bullard, M.; Zeitz, H.-G. *Synlett* **1991**, 425. (c) Crich, D.; Davies, J. W. *Tetrahedron* **1989**, *45*, 5641. (d) Ogura, K.; Yanagisawa, A.; Fujino, T.; Takahashi, K. *Tetrahedron Lett.* **1988**, *29*, 5387. (e) Crich, D.; Davies, J. W. *Tetrahedron Lett.* **1987**, *28*, 4205. (f) Vassen, R.; Runsink, J.; Scharf, H.-D. *Chem. Ber.* **1986**, *119*, 3492. (g) Henning, R.; Urbach, H. *Tetrahedron Lett.* **1983**, *24*, 5343. (h) Curran, D. P.; Thoma, G. *Tetrahedron Lett.* **1991**, *32*, 6307. (i) Curran, D. P.; Abraham, A. C.; Liu, H. *J. Org. Chem.* **1991**, *56*, 4335. (j) For the addition of tris(trimethylsilyl)silyl radicals to chiral ketones, see: Giese, B.; Damm, W.; Dickhaut, J.; Wetterich, F.; Sun, S.; Curran, D. P. *Tetrahedron Lett.* **1991**, *32*, 6097. (k) Arya, P.; Lesage, M. Submitted for publication (personal communication).
(4) (a) Guindon, Y.; Yoakim, C.; Lemieux, R.; Boisvert, L.; Delorme, D.; Lavallée, J.-F. *Tetrahedron Lett.* **1990**, *31*, 2845. (b) Guindon, Y.; Lavallée, J.-F.; Boisvert, L.; Chabot, C.; Delorme, D.; Yoakim, C.; Hall, D.; Lemieux, R.; Simoneau, B. *Tetrahedron Lett.* **1991**, *32*, 27. (c) For examples of chelation-controlled radical reductions, see: Guindon, Y.; Lavallée, J.-F.; Llinas-Brunet, M.; Horner, G.; Rancourt, J. *J. Am. Chem. Soc.* **1991**, *113*, 9701.

0002-7863/92/1514-4912$03.00/0